

Lumping and Reduction of Detailed Kinetic Schemes: an Effective Coupling

Alessandro Stagni, Alberto Cuoci, Alessio Frassoldati, Tiziano Faravelli, and Eliseo Ranzi*

Department of Chemistry, Materials, and Chemical Engineering, Politecnico di Milano P.zza Leonardo da Vinci 32, 20133 Milano, Italy

1. INTRODUCTION

In the latest decades, the increasing need of an optimal design of combustion devices, as well as the control of pollutant emissions, has led to the development of numerical models in support of experimental research. The reliability of these models depends on a variety of factors; among them, the accurate description of the combustion chemistry through proper kinetic models takes a significant importance. For this reason, detailed kinetic schemes have been developed, which describe the elementary steps occurring within the combustion process. Indeed, as pointed out by Lu and Law,¹ the use of partial equilibrium chemistry or one-step overall reaction is often too simplistic for accurately describing reacting flows. As a consequence, several mechanisms were proposed and validated in the latest 20 years and many of them for primary fuels and surrogates are available in the literature.^{2–5} As already discussed by Huang et al.,⁶ comprehensive descriptions of combustion systems frequently contain large numbers of species and reactions, making the prediction of chemical kinetics computationally expensive, particularly when the aim is to embody them within computational fluid dynamic models. Therefore, there is a need for the development of mathematical representations of chemical kinetics that maintain the important features of full schemes, but with higher computational efficiency and reduced numbers of variables.

In contrast to a potentially higher degree of accuracy, the development and application of a detailed kinetic mechanism introduces several issues, too. In particular, two of them are summarized here:

- The dimensions of a detailed mechanism become easily unbearable, as its size grows exponentially with the size of the involved fuels. Altgelt and Boduszynski⁷ calculated that, if all the branched alkane isomers are considered, the number of involved molecules may be higher than hundreds of thousands if compounds up to C_{20} are considered. If one also considers that liquid fuels also include cyclo-alkanes and aromatics, it becomes clear that the resulting number of species is not acceptable. Moreover, it has been shown that detailed chemistry of large unsaturated species generates a huge and unmanageable number of species;⁸
- The high number of involved compounds results in an even higher number of reactions. Lu and Law¹ empirically showed a quasi linear proportionality

Received: October 3, 2013

Revised: November 25, 2013

Accepted: November 25, 2013

Published: November 25, 2013

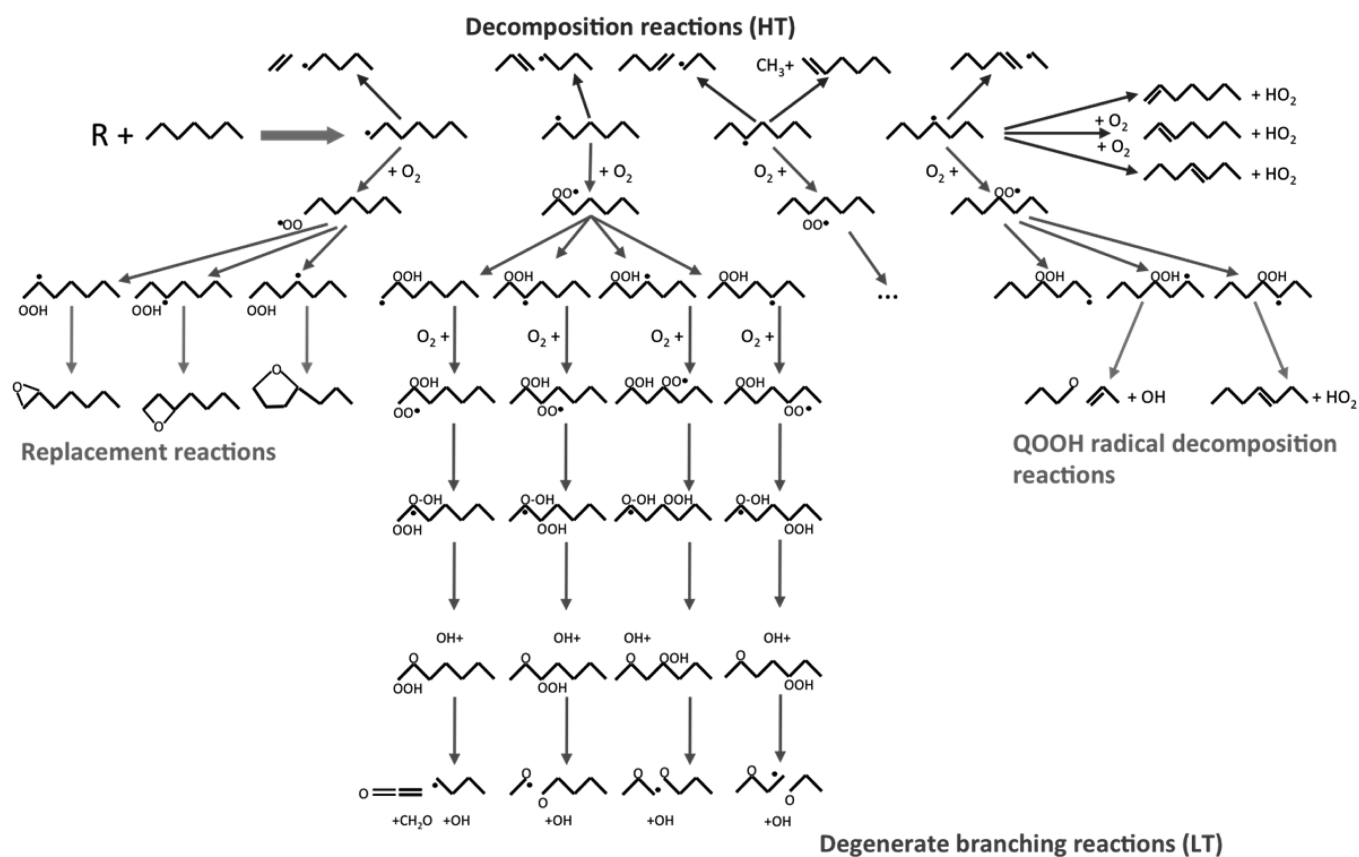


Figure 1. *n*-Heptane oxidation mechanism. Primary propagation reactions of *n*-heptane.

between species and reactions in detailed mechanisms, with the number of reactions usually 4–5 times higher than the number of species. This dimension means that a manual compilation of a detailed scheme is not practical, and automatic generation of detailed schemes becomes a need for the combustion characterization of large fuels.

In order to overcome these difficulties, several solutions were proposed.¹ Among them, lumping techniques take a leading role: starting from a detailed mechanism, lumping methods^{6,9,10} group more compounds (isomers) in one single pseudospecies, thus reducing the overall number of constitutive equations of the related models. In this way more handful mechanisms, easier to be used during the whole validation process, are obtained, because of the significantly lower computational cost. Nevertheless, in the case of very complex simulations, like those often encountered in CFD applications, the size of the mechanism is still excessive, and a further reduction is then needed.

In this paper this issue is faced, and a novel strategy to make the problem manageable is proposed. Starting from the automatic generation of detailed kinetic schemes through the identification and selection of different reaction classes, the chemical lumping procedures are briefly summarized. Afterward, the lumped kinetic models of *n*-heptane and *n*-dodecane oxidation are discussed and also validated through a comparison with experimental data and simulation results of a detailed kinetic model. A new and simple strategy of mechanism reduction is then presented and applied in order to reduce the lumped kinetic models. Finally, the performances of the obtained reduced mechanisms are assessed in the last two sections, where their predictions are compared to experimental

data and a multidimensional application of the reduced scheme to laminar coflow flames is presented. In this way, the reliability and the suitability of this coupling of lumping and reduction techniques is shown.

2. AUTOMATIC GENERATION OF CHEMICAL MECHANISMS

For several years now, a pioneering approach toward the automatic generation of reaction mechanisms and applications to the modeling of engine knock was proposed by Westbrook et al.¹¹ and by Chevalier et al.¹² General rules of LISP language¹³ were applied to identify the chemical species produced, the reactions between these species and the elementary reaction rates for each reaction step. The low temperature reaction mechanism for several alkane fuels up to cetane (*n*-hexadecane) involves two successive additions of radicals to oxygen and the formation of alkenes, cyclic ethers, and a very reactive hydroketoperoxide. These oxidation mechanisms were used for predicting knock tendencies in internal combustion engines, without considering product distribution and successive reactions. The automatic generation of primary oxidation reactions of *n*-alkanes and large hydrocarbon fuels was then further investigated in several different papers.^{14–20} All the possible reactions were classified and written for alkyl, peroxyalkyl, and hydroperoxyalkyl radicals. The only simplification was globalizing the successive isomerization and decomposition reactions leading to the formation of branching agents from peroxyalkylhydroperoxy radicals into a single reaction after the second oxygen addition.²¹ As a result of this activity, *n*-heptane oxidation mechanisms were thus presented and extensively validated.^{15,22–24} Figure 1 shows

the low temperature oxidation mechanism of *n*-heptane¹⁵ and is a clear example of the complexity of these reaction schemes.

Excellent reviews on the detailed chemical kinetic models for low and high temperature combustion of hydrocarbon fuels^{25–27} allowed to better highlight the different reaction classes involved in these low and high temperature mechanisms.²⁸ On these bases, combustion mechanism of *n*-heptane was easily extended and validated to heavier species up to *n*-cetane.^{4,29} Large *n*-alkanes display the same kinetic behavior of *n*-heptane in both the high- and the low-temperature regions and allow a direct extension of the overall kinetic model to species up to *n*-hexadecane. There are 362 primary propagation reactions of *n*-hexadecane, involving 100 different radicals (alkyl: R, peroxy: ROO, hydroperoxyalkyl: QOOH, and hydroperoxyalkylperoxy: OOQOOH) and 80 primary parent molecules always retaining 16 C atoms (alkenes, ethers, hydroperoxides, and carbonyl-hydroperoxides). The detailed description of successive reactions of all these new intermediate species rapidly makes an overall detailed mechanism scarcely manageable.

According to Westbrook et al.,⁴ the mechanism for *n*-hexadecane includes 8130 elementary reversible reactions among 2116 chemical species, and these totals increase when additional submechanisms are added, such as a reasonably complete NOx or soot submodel. The sizes of some of the fuel mechanisms from C10 through C16 when species and reactions for larger fuels have been removed are indicated in Table 1.

Table 1. Number of Species and Reactions in Different LLNL Fuel Mechanisms⁴

	C ₁₆ H ₃₄	C ₁₄ H ₃₀	C ₁₂ H ₂₆	C ₁₀ H ₂₂
reactions	8130	6449	5030	3878
species	2116	1668	1282	940

These values do not account for possible pyrolysis reactions to form aromatics and heavy unsaturated species. As a consequence, the kinetic modeling of large molecules benefits significantly from simplifications and semidetailed approaches.

3. CHEMICAL LUMPING PROCEDURES

As already summarized by Huang et al.,⁶ species lumping was and is extensively and effectively used to model reduction, with applications in pyrolysis, combustion, and atmospheric chemistry.^{10,30–33} The crucial issues in this approach are (i) to determine which species are to be lumped; (ii) to classify how the selected species should contribute to the lumped species, i.e., define the lumping transformation; and (iii) to estimate kinetic parameters for the lumped species. There are basically two different lumping approaches. First there are chemical lumping methods where species are organized into lumps according to their chemical structure or reactivity.^{10,30} This approach is theoretically sound but requires extensive chemical expertise to organize the lumping structures. Then there are mathematically based approaches in which formal rules for transforming between original and lumped variables are defined.^{6,32,34}

While an extensive discussion on chemical lumping procedures adopted in pyrolysis and combustion systems is already reported elsewhere,^{10,29} here we shortly summarize the main features of this approach. At high temperatures, the interactions between large alkyl radicals and the reacting mixture are very weak and this fact allows the direct

substitution of these radicals with their primary isomerization and decomposition products. In principle, heavy radicals could also undergo H-abstraction, addition on unsaturated bonds, and recombination reactions. Due to the limited weight of these reactions compared to the isomerization and decomposition ones, it is possible to drastically reduce the total number of radicals and reactions to be considered. All of the intermediate alkyl radicals higher than C₄ are supposed to be instantaneously transformed into their final and more stable products. On the basis of the steady state approximation, continuity equations of heavy radicals allow to directly deduce the apparent stoichiometry of their decomposition path.^{10,29} Large sections of the kinetic scheme can be reduced to a few equivalent or lumped reactions while still maintaining a high level of accuracy. Similarly, in the low temperature mechanism, the lumped approach here adopted groups together the four classes of primary intermediate radicals. Similarly, the isomers of the primary products, such as alkenes, cyclic ethers, and carbonyl hydroperoxides are also grouped into single corresponding species. To better illustrate this simplification, Figure 2 shows the lumped oxidation mechanism of *n*-dodecane.

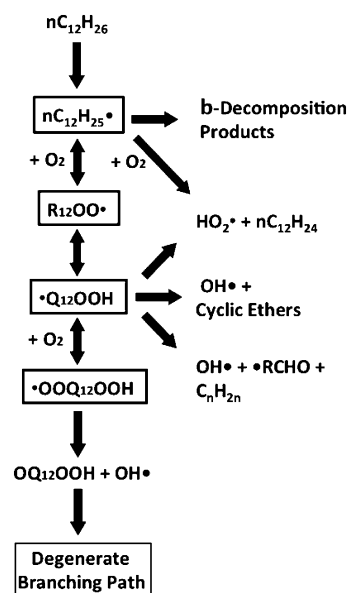


Figure 2. Lumped oxidation mechanism of *n*-dodecane.

Thus, the 6 alkyl, 6 peroxy, 30 hydroperoxyalkyl, and 30 hydroperoxyalkylperoxy radicals are simply grouped into 4 lumped radicals: R₁₂, R₁₂OO, Q₁₂OOH, and OOQ₁₂OOH. Similarly, the 6 alkenes, 16 O-heterocycles, 6 hydroperoxides, and 30 carbonyl-hydroperoxides only refer to 4 lumped components. In this way, a limited number of lumped intermediate components makes the comprehensive description of their successive reactions easier and more viable. This approach has already been successfully adopted for several years.

In her review of low temperature experiments and kinetic models, Battin-Leclerc²⁶ already carried out a discussion and comparison of lumped and detailed kinetic models. The next paragraph will shortly present some comparisons of experimental data of the oxidation of *n*-heptane and *n*-dodecane and model predictions.

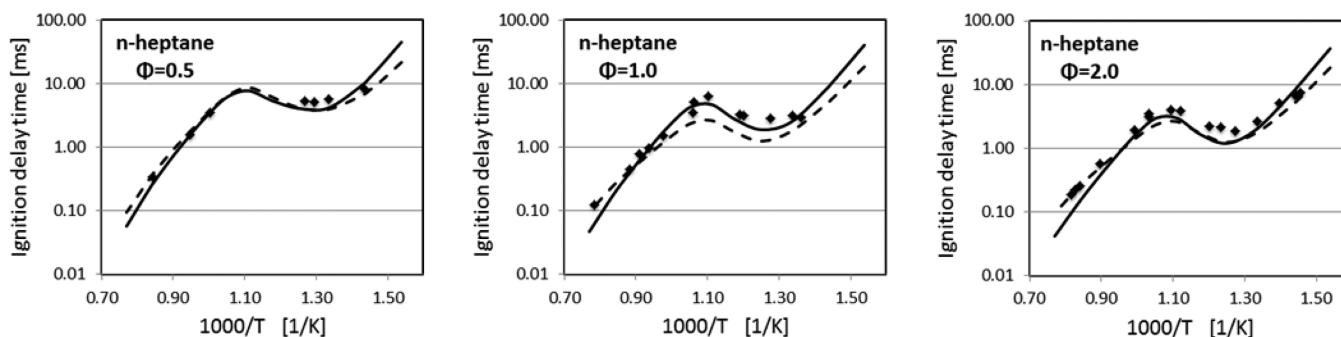


Figure 3. *n*-Heptane/air ignition delay times at 13.5 atm. Comparison of experimental data³⁶ (symbols) and predictions of the detailed (dashed lines) and lumped mechanisms (solid lines).

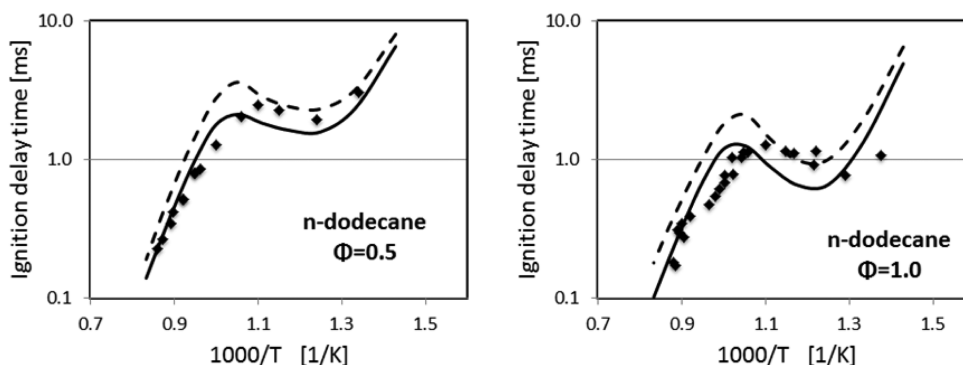


Figure 4. *n*-Dodecane/air ignition delay times at 20 atm. Comparison of experimental data³⁷ (symbols) and predictions of the detailed (dashed lines) and lumped mechanisms (solid lines).

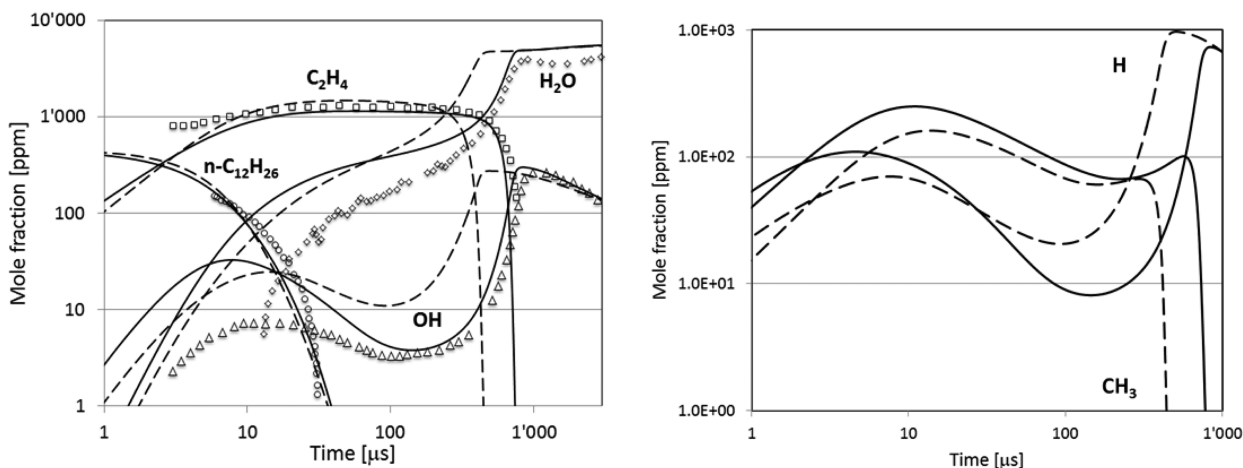


Figure 5. Species time history for *n*-dodecane oxidation. Nominal initial conditions: 1410 K, 2.3 atm, 457 ppm *n*-dodecane/O₂/argon, $\Phi = 1$. Comparison of experimental data (symbols) and predictions of the detailed (dashed lines) and lumped scheme (solid lines).³⁸

4. VALIDATION OF THE LUMPED KINETIC SCHEMES OF *N*-HEPTANE AND *N*-DODECANE OXIDATION

The kinetic models of *n*-heptane and *n*-dodecane oxidation are here considered as a useful example in order to show the main characteristics of their successive reduction process. This selection is mainly due to the interest of these fuels, as primary reference components in gasoline and liquid fuels, as well as to the availability of these schemes in the open literature. The extension of the oxidation mechanism up to *n*-dodecane and also *n*-cetane was always made on the basis of the same reaction classes already discussed and considered in *n*-heptane kinetics.²⁴ Thus, we will refer to the lumped model developed at Politecnico di Milano³⁵ (POLIMI_1212 is freely available on

<http://creckmodeling.chem.polimi.it/>), as well as to the detailed kinetic scheme of Lawrence Livermore National Laboratory (LLNL),⁴ for further comparisons. The validation of both the kinetic models has already been carried out and extensively discussed in the previously referred papers.^{4,35} Nonetheless, in order to compare the performance between detailed and lumped schemes, a few examples are here reported also in order to better analyze and discuss the performances of the corresponding reduced schemes.

Thus, Figures 3 and 4 show the comparisons between predicted and experimental ignition delay times of *n*-heptane³⁶ and *n*-dodecane,³⁷ respectively. The comparisons refer to experimental data (symbols) and both to LLNL (solid line) and

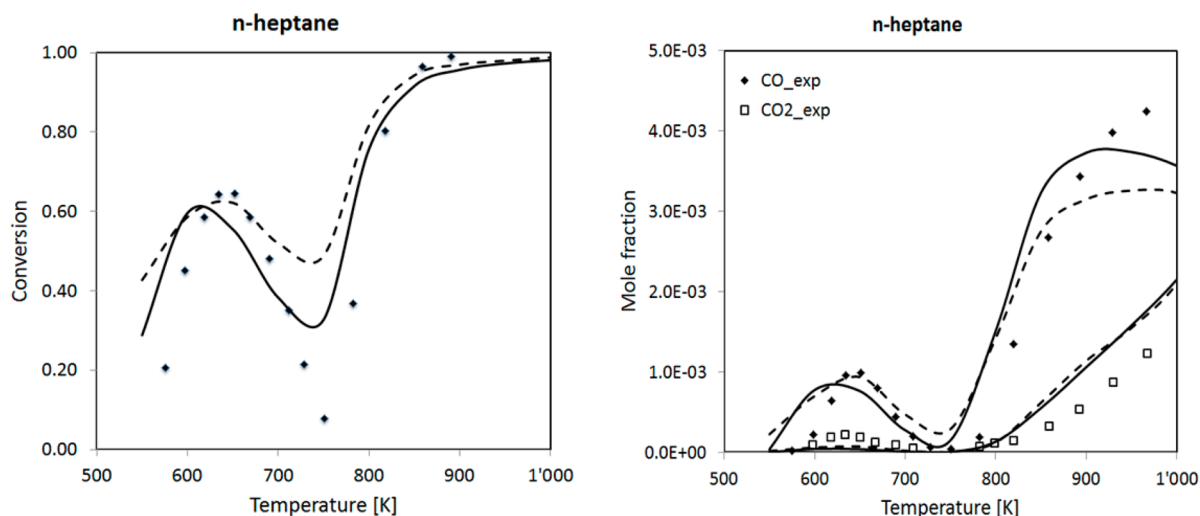


Figure 6. *n*-Heptane oxidation in a jet stirred reactor at high pressure ($P = 10$ bar) and at a constant residence time (τ) of 1 s.⁵⁷ Comparison of experimental data (symbol) and predictions of the detailed (dashed lines) and lumped mechanisms (solid lines).

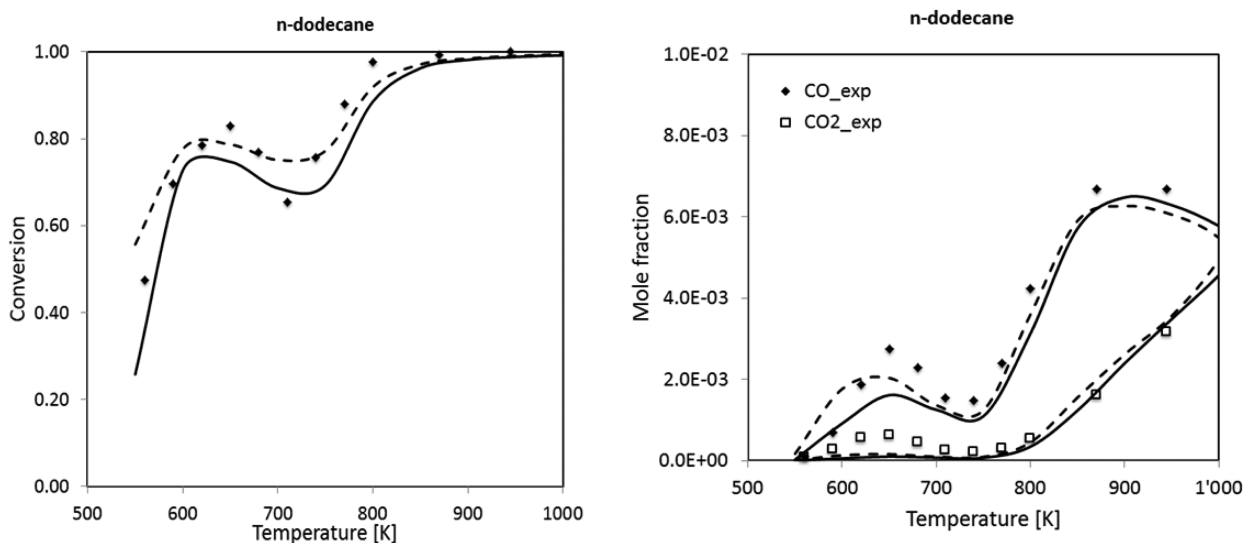


Figure 7. *n*-Dodecane oxidation in a jet stirred reactor at high pressure ($P = 10$ bar) and at a constant residence time (τ) of 1 s. Comparison of experimental data⁴⁰ (symbols) and predictions of the detailed (dashed lines) and lumped mechanisms (solid lines).

POLIMI kinetic scheme (dashed lines). These comparisons of ignition delay times of *n*-alkanes confirm that both the kinetic models properly account for the low and high temperature mechanisms for both the *n*-alkanes. The deviations between the detailed and the lumped kinetic scheme fall within the experimental uncertainties. Moreover, it is important to highlight that these deviations are also due to the different C_1 – C_4 mechanism, especially at high temperatures.

Recently, ignition delay times and multispecies time histories were measured by Davidson et al.³⁸ during *n*-dodecane oxidation behind reflected shock waves using a heated, high-pressure shock tube. The comparisons in Figure 5 show the similar prediction capabilities of both the kinetic schemes, also with respect to intermediate and radical species. Furthermore, Figures 6 and 7, where *n*-heptane and *n*-dodecane oxidation in jet stirred reactor is analyzed,^{39,40} confirm the similarity of the two schemes. Again, deviations are within the experimental uncertainties. The behavior of other products is giving very similar information, for this reason further comparisons are not reported.

Finally, Figures 8 and 9 show a comparison of the experimental data of the laminar flame speed of *n*-heptane and *n*-dodecane, respectively, with the predictions of POLIMI kinetic scheme. A similar comparison with the detailed LLNL scheme could not be directly obtained, without a preliminary reduction phase for computational reasons. Thus, when studying the extinction strain rates of laminar flames of heavy *n*-alkanes, Li et al.⁴¹ superimposed onto JetSurF 2.0⁴² a skeletal version of the detailed kinetic model of *n*-alkane oxidation of Westbrook et al.⁴ Similarly, in the very recent work of Zhang and Egolfopoulos,⁴³ the kinetic analysis of *n*- and *iso*-cetane laminar flame speeds was carried out only by using the lumped kinetic scheme.

This validation and all the comparisons both with experimental data and with the predictions of the detailed kinetic model confirm the reliability of the lumped kinetic model which will be used as reference for the following discussion on mechanism reduction.

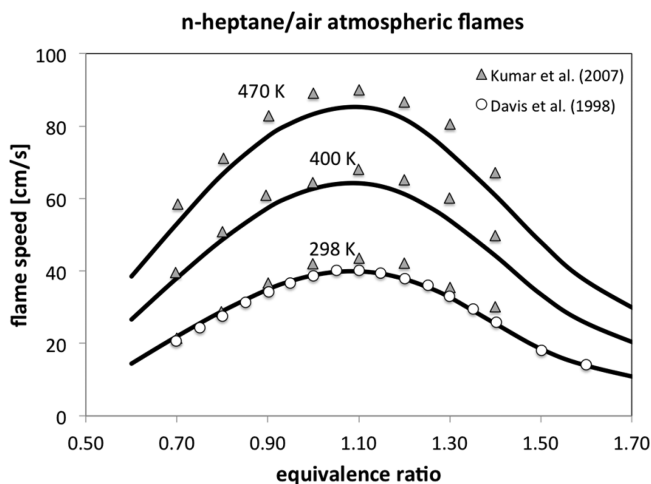


Figure 8. Laminar speeds of *n*-heptane/air atmospheric flames. Experimental data from Kumar et al.⁵⁸ and Davis et al.⁵⁹

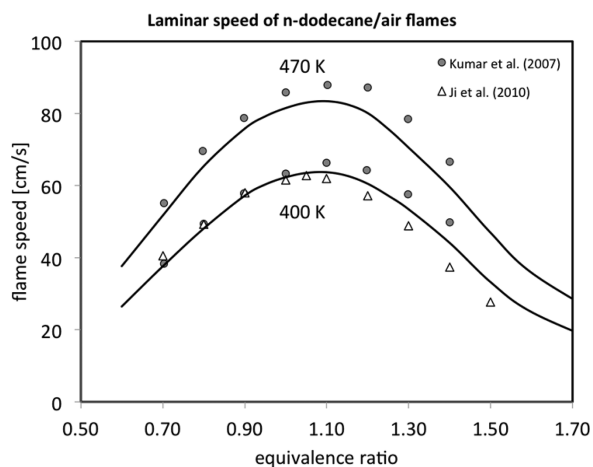


Figure 9. Laminar speeds of *n*-dodecane/air atmospheric flames. Experimental data from Kumar et al.⁵⁸ and Ji et al.⁶⁰

5. AUTOMATIC REDUCTION OF KINETIC SCHEMES

As pointed out by Lu and Law,¹ while earlier reduction methods were mainly based on manual output analysis, the current techniques rely on automatic simplifications of the original kinetic schemes. These methods identify the unimportant reactions and species by focusing on different parameters. The reduction method of Wang and Frenklach⁴⁴ identifies the unimportant reactions by comparing the reaction rates with that of a preselected controlling reaction, which is properly chosen as a reference. Other methods are targeted at the reduction of the number of species. For instance, the method of directed relation graph (DRG) developed by Lu and Law⁴⁵ identifies the different couplings among the species. Once a set of “important” species is identified upstream, the relative contribution of each of the remaining species of the detailed mechanism to the production rate of the important species is quantified: if and only if it is significant, these species are kept; otherwise, they are not considered in the reduced mechanism. In this way, the DRG method reduces the number of mass balance equations.

The reduction method applied in this work is based on the analysis of reacting fluxes within different combustion systems. As already discussed elsewhere,⁴⁶ the first point is to define the

range of operating conditions required for the reduced scheme. Here we select temperature, pressure, and composition (i.e., equivalence ratio) in such a way to cover the typical operating conditions encountered in internal combustion engines during a whole engine cycle. For *n*-heptane and *n*-dodecane oxidation in air, the adopted range of operating conditions is reported in Table 2.

Table 2. Range of Operating Conditions Adopted in the Present Work to Reduce the Detailed Kinetic Mechanisms of *n*-Heptane and *n*-Dodecane

	range
temperature	700–2000 K
pressure	1–50 atm
equivalence ratio	0.25–3.0

Once the values of these three operating variables are chosen, their combinations allow to define, for instance, the initial conditions of different plug flow reactors (PFR). For each reactor simulation, a rate of production analysis is performed to calculate the total flux of each species. This is built up starting from the absolute reaction rate of each species throughout the reactor length, evaluated locally as

$$R_i = \sum_{j=1}^{N_R} |\nu_{i,j} r_j| \quad (1)$$

where $\nu_{i,j}$ are the stoichiometric coefficients of the *i*th species in the *j*th reaction, r_j is the net rate of the *j*th reaction. The total flux of each species is obtained as the integration of eq 1 over the PFR length:

$$F_i = \int_0^{t_j} R_i dt \quad (2)$$

For each reactor simulation, the obtained values of F_i are normalized with respect to the local maximum value in such a way that all the PFRs have the same importance in the evaluation of the overall reacting fluxes. Then, the integral fluxes of all the reactors are summed up and sorted in a descending order. In this way, according to the desired number of species in the reduced mechanism, only the first *n* species are kept. Afterward, a reaction is retained in the reduced scheme if and only if all the involved species belong to the set of the first *n* species; otherwise, it is discarded. In this way the reduced kinetic scheme is obtained. Compared to other reduction approaches, this method is peculiar because it does not need to define an a priori list of important species. Of course, it is possible to force the presence of specific species, like in the case of nitrogen or different inert species.

Through this approach, several reduced models, both of *n*-heptane and *n*-dodecane oxidation, were obtained by considering the same set of PFR conditions and starting always from the original lumped schemes (POLIMI_1212). In the following, nC7_NS-species and nC12_NS-species indicate the reduced models with NS species, respectively, for *n*-heptane and *n*-dodecane.

Originally, the lumped kinetic scheme POLIMI involves 435 species and is very general and able to describe the pyrolysis and oxidation of a large set of hydrocarbon and oxygenated fuels and their mixtures.⁴⁷ For this reason, an important part of the removed species simply are fuels and oxygenated species not belonging to the combustion paths of hydrocarbon species.

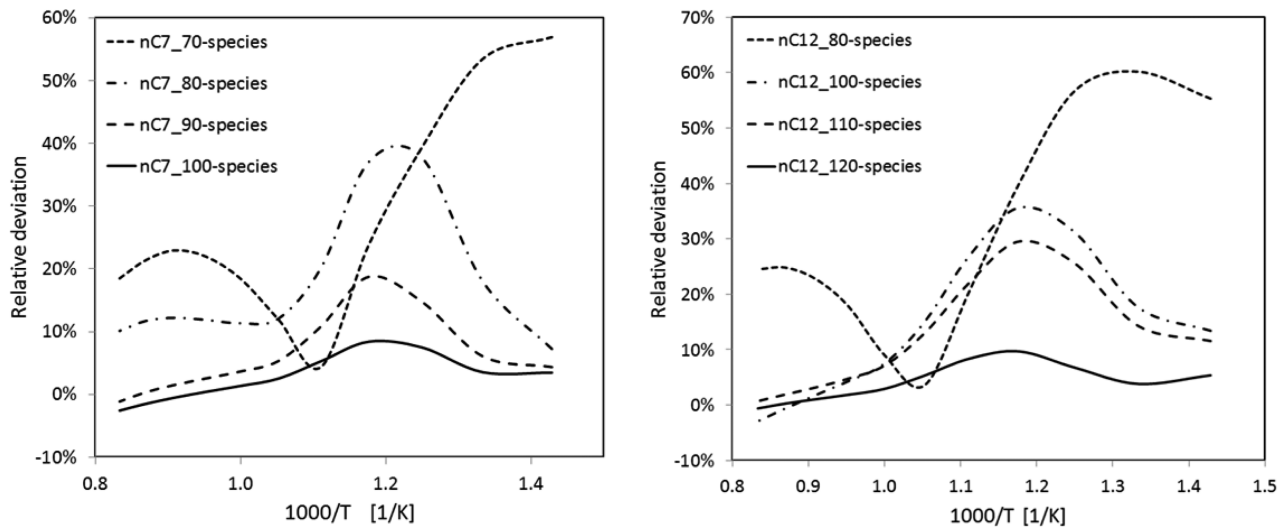


Figure 10. Relative deviations of the ignition delay times of different reduced schemes with respect to the reference mechanism of *n*-heptane (left) and of *n*-dodecane (right).

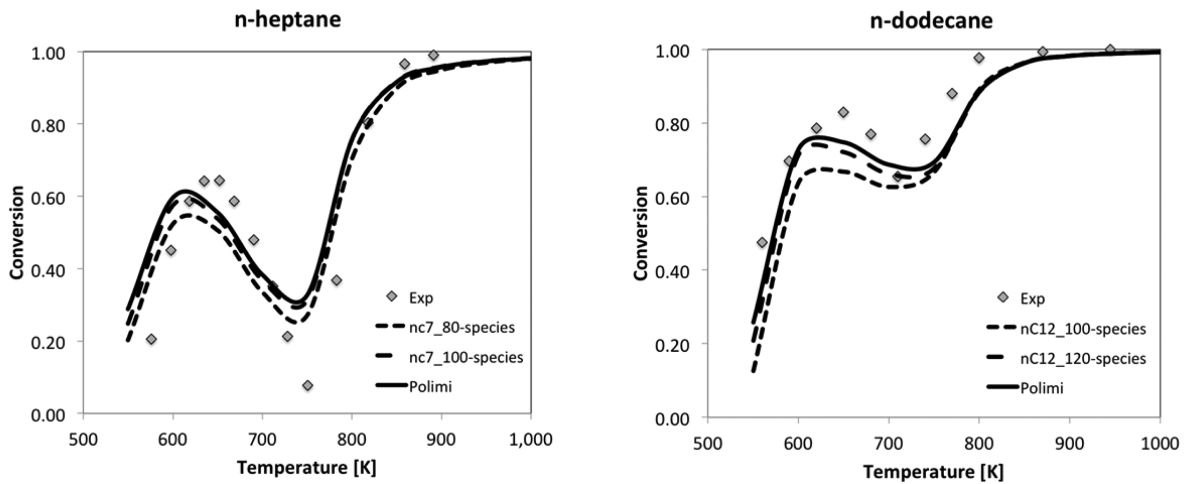


Figure 11. *n*-Heptane and *n*-dodecane conversion in the jet stirred reactor of Figures 6 and 7. Comparisons of experiments (symbols) and original and reduced schemes (lines).

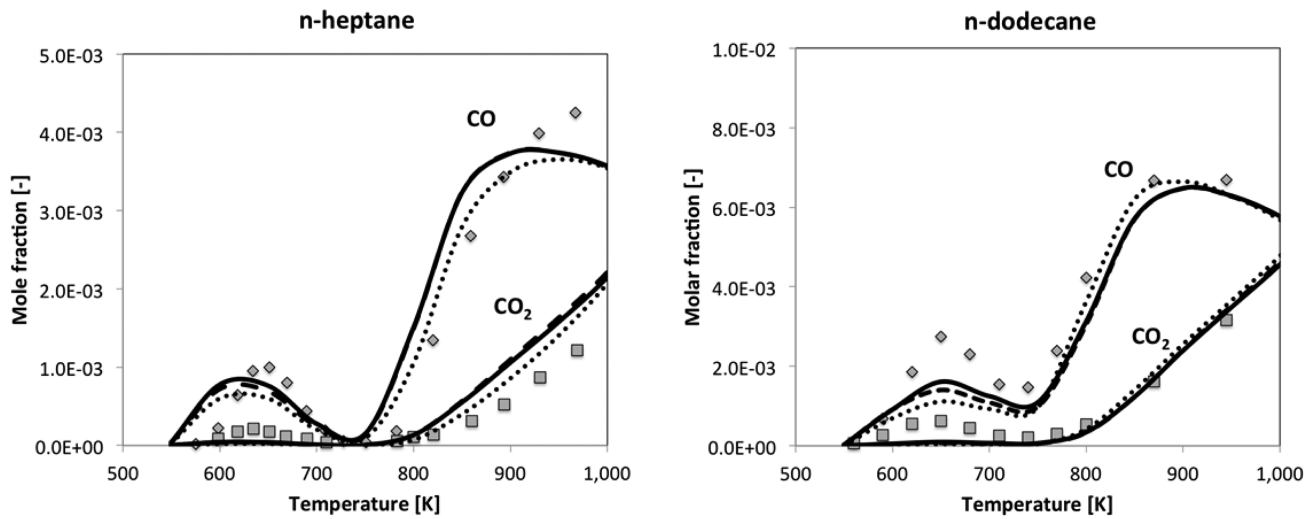


Figure 12. CO and CO₂ profiles in the jet stirred reactor of Figures 6 and 7. Comparisons of experiments (symbols) and original and reduced schemes (lines).

6. REDUCED KINETIC SCHEMES OF *N*-HEPTANE AND *N*-DODECANE OXIDATION AND MECHANISM VALIDATION

On the basis of the previous reduction method, applied to the same set of selected operating conditions, several reduced kinetic schemes were derived for both the fuels. By simply assuming a maximum error of 10% on the ignition delay times of the overall set of shock tube experiments, the reduced kinetic schemes of *n*-heptane and *n*-dodecane oxidation are constituted by 120 and 100 species, respectively. The full detail of species and reactions, in CHEMKIN format, are reported as Supporting Information (thermodynamic and transport properties are available on <http://creckmodeling.chem.polimi.it/>).

Figure 10 shows the relative deviations of the ignition delay times of different reduced schemes with respect to the reference mechanism, both for *n*-heptane and for *n*-dodecane. These deviations refer to the stoichiometric conditions already reported in Figures 3 and 4 for *n*-heptane and *n*-dodecane, respectively. Similar deviations are also observed in the overall set of shock tube experiments.

As a further comparison of the reduced scheme with the original one, Figure 11 reports the *n*-heptane and *n*-dodecane conversion in the jet stirred reactor of Figures 6 and 7, respectively. Also, Figure 12 shows a similar comparison of the CO and CO₂ profiles.

Figure 13 not only shows that the 120-species reduced model of *n*-dodecane oxidation agrees well with experiments and the

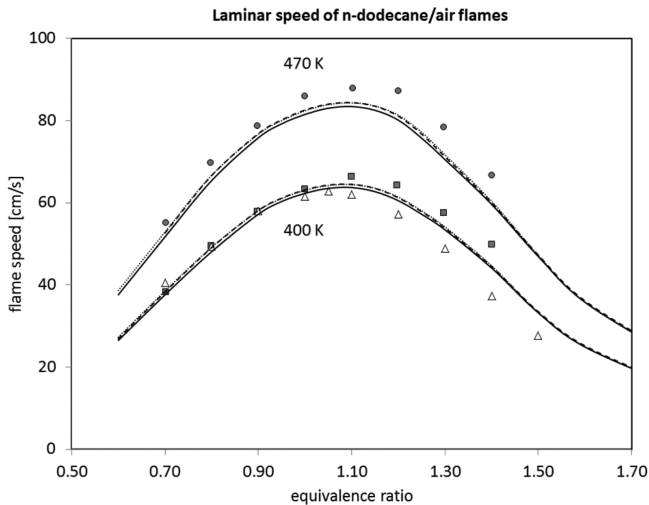


Figure 13. Laminar speed of *n*-dodecane/air flames. Comparisons of experimental data^{58,60} (symbols) with predictions of the original lumped model (solid lines), the 120-species reduced model (dashed lines), and a 100-species reduced model (dotted lines).

original mechanism, but it also points out that the scheme can be further reduced when the target is modeling laminar flame speeds. As a matter of fact, it is well-known that flame speed is scarcely affected by fuel specific reactions;^{35,43} therefore, all the low temperature mechanism and related species can be removed without a significant effect on predicted values. Indeed, both the 120- and 100-species reduced schemes show the same behavior in this regard, although their performances in predicting ignition delays are quite different. Figure 14 shows a similar comparison for the high temperature shock ignition already analyzed in Figure 5³⁷ and confirms this behavior.

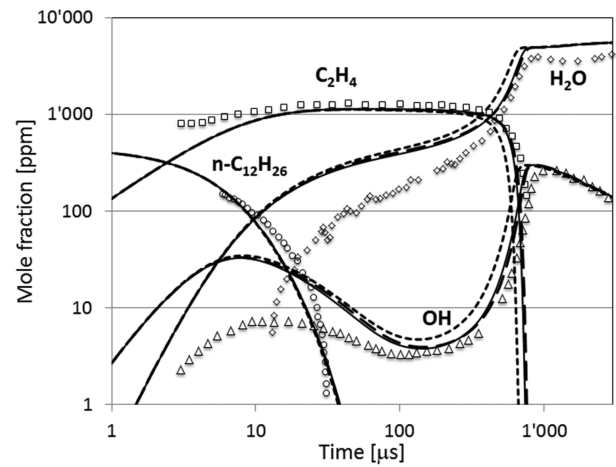


Figure 14. Time histories of radical and major species in *n*-dodecane oxidation. Comparisons of experimental data³⁸ (symbols) with predictions of the original lumped model (solid lines), the 120-species reduced model (dashed lines), and a 100-species reduced model (dotted lines).

7. MULTIDIMENSIONAL APPLICATION: MODELING OF LAMINAR, COFLOW FLAMES

In order to better show the benefits and the importance of reducing detailed kinetic schemes for practical applications, we performed numerical simulation of multidimensional laminar flames, comparing the reduced kinetic mechanisms of *n*-heptane and *n*-dodecane described in the previous sections with the original lumped kinetic mechanism. The laminar conditions are chosen in order to avoid the additional complexity associated to the numerical modeling of the effects of turbulence on the chemistry. Moreover, the attention is focused on a multidimensional system to better show the computational advantages of the proper reduction of kinetic schemes in real applications, where the interaction of chemistry with complex fluid dynamics is always present.

A couple of coflow, axisymmetric, laminar diffusion flames, fed with *n*-heptane and *n*-dodecane respectively, are numerically studied (Figure 15). A burner with two concentric inlet streams, with diameters of 2.41 and 25.4 mm for the fuel and

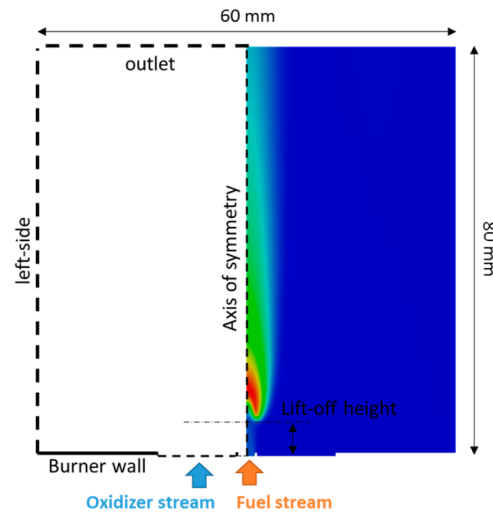


Figure 15. Coflow, laminar diffusion flames: schematic of the diffusion flame setup, together with dimensions of the computational domain.

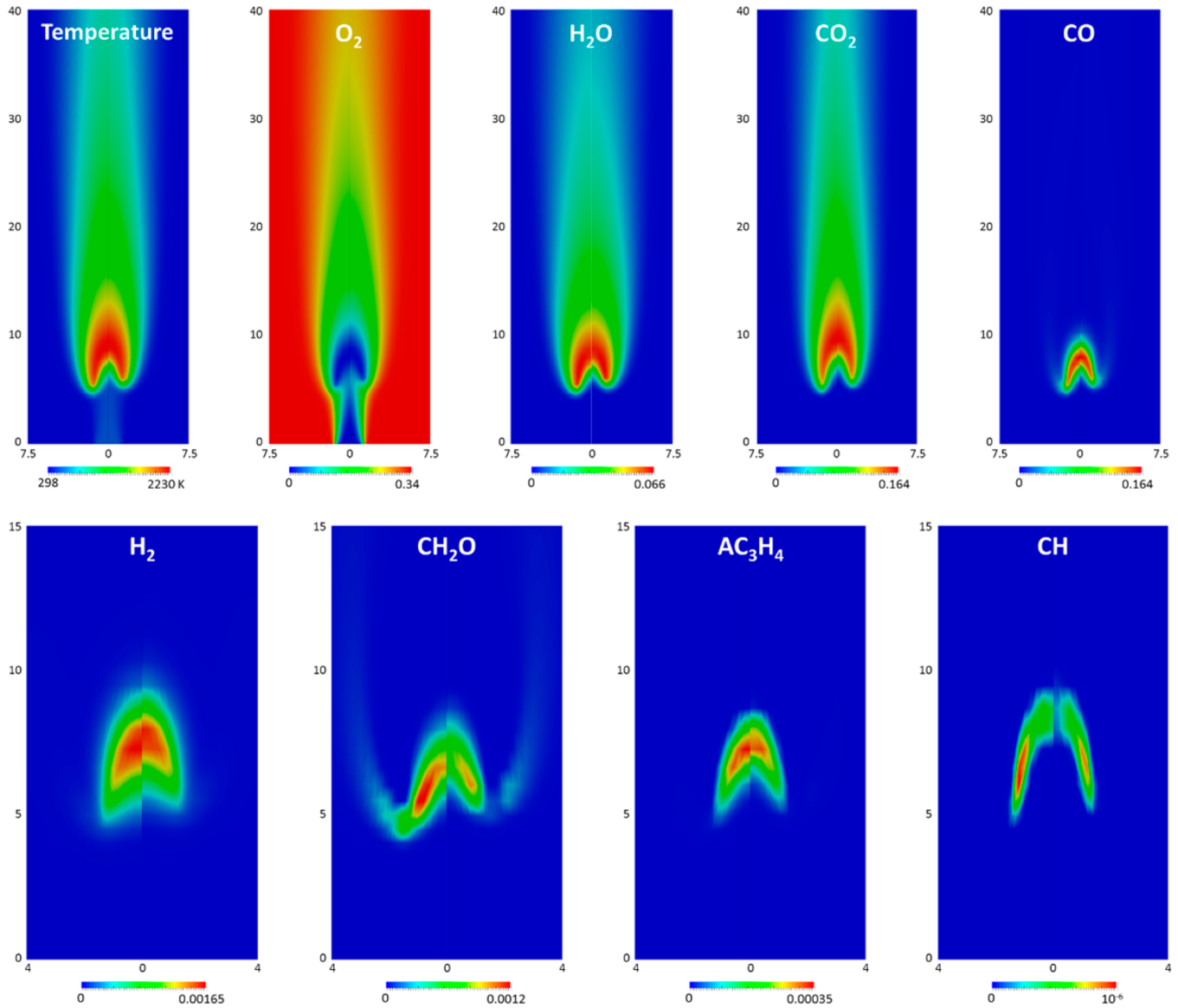


Figure 16. Calculated maps of temperature and mass fractions of selected species for the coflow flame fed with *n*-heptane. The left side of each map refers to the simulation performed using the reduced kinetic mechanism for *n*-heptane, while the right side corresponds to the simulation performed using the original kinetic mechanism. The coordinates along the axial and radial directions are in millimeters.

oxidizer streams, is considered. A parabolic, fully developed velocity profile is assumed for the inner fuel stream, with an average value of 79 cm/s. A top-hat profile is imposed for the outer oxidizer stream, with an average speed of 68.7 cm/s. The fuel stream is a mixture of 3.67% of fuel (*n*-heptane or *n*-dodecane) and 96.33% of nitrogen, by volume. The outer stream is oxygen-vitiated air with 31% of oxygen. The fuel stream is injected at 470 K, while the oxidizer stream at ambient temperature. The same burner geometry was extensively adopted by Tosatto et al.⁴⁸ to perform experimental and numerical studies of coflow flames fed with JP8 surrogates. In the present work, we simply replaced the inlet fuel with *n*-heptane or *n*-dodecane, by keeping fixed all the remaining boundary conditions. This particular burner geometry was chosen since the resulting laminar flames show a lift-off height. As reported by Mohammed et al.,⁴⁹ the ability to correctly capture the flame lift-off from a computational point of view is strongly dependent on the reliability and accuracy of the kinetic scheme. Therefore, such kind of flames appears a convenient

choice to investigate the quality of the reduced kinetic mechanisms.

The numerical simulations of the flames described above require the solution of the following steady-state equations, in a 2D axisymmetric computational domain:

- the Navier–Stokes equations, for the conservation of mass and momentum;
- the conservation equation of energy, recast in the temperature form;
- a conservation equation for each species in the adopted kinetic scheme, accounting for convection, diffusion and reaction.

The equations above need proper boundary conditions. In particular, at the inlets of fuel and oxidizer streams, Dirichlet conditions are imposed, to fix velocity, temperature, and composition. At the centerline, symmetry conditions are adopted and homogeneous Neumann conditions are imposed to model the outflow conditions at the top of the computa-

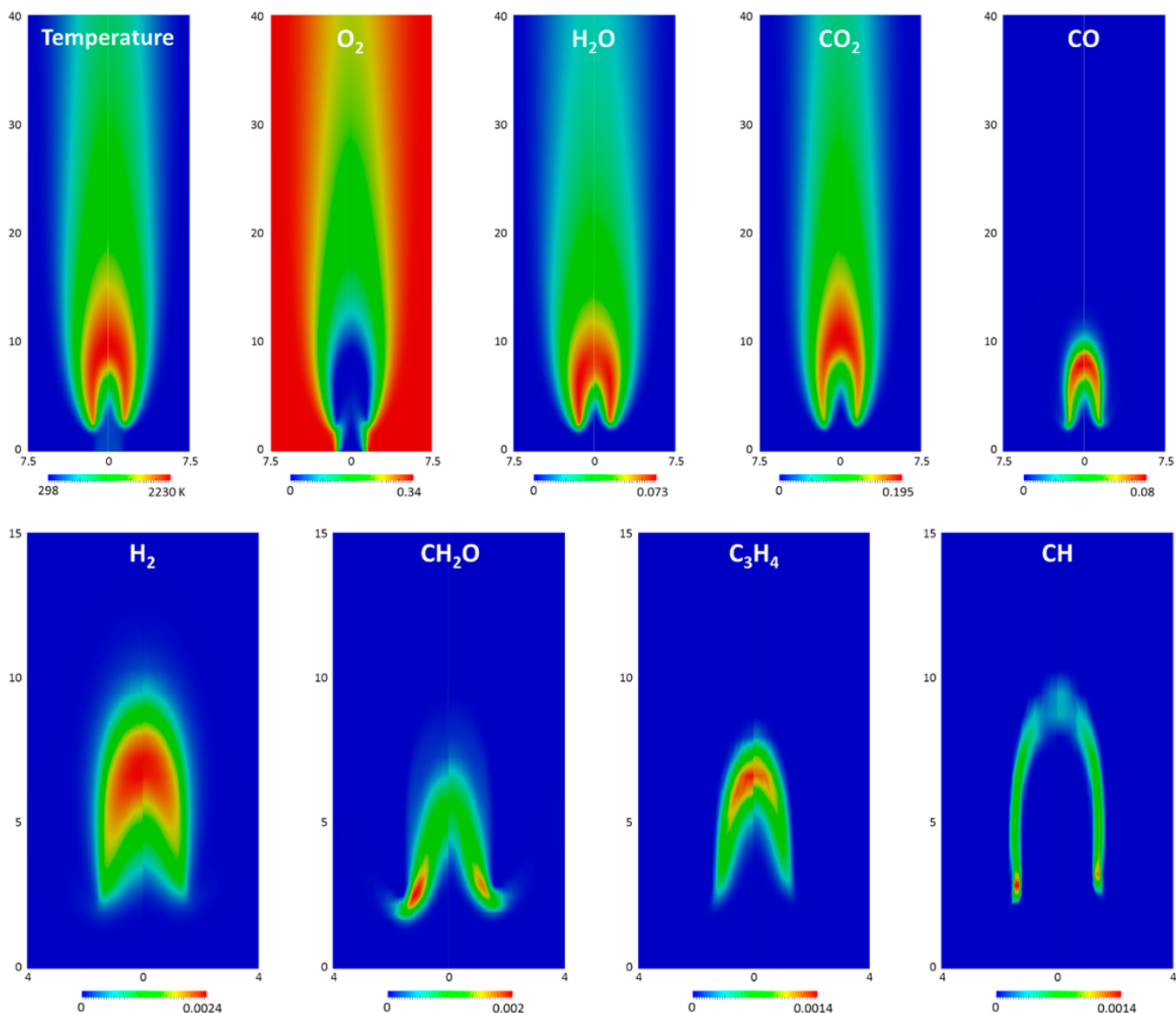


Figure 17. Calculated maps of temperature and mass fractions of selected species for the coflow flame fed with *n*-dodecane. The left side of each map refers to the simulation performed using the reduced kinetic mechanism for *n*-dodecane, while the right side corresponds to the simulation performed using the original kinetic mechanism. The coordinates along the axial and radial directions are in millimeters.

tional domain. A 2D rectangular computational domain was chosen, with size equal to 30 mm \times 80 mm, which is sufficiently large to ensure that the boundary conditions do not affect the flame region. A nonuniform, structured mesh with 120 points along the axis and 50 points along the radial coordinate was adopted to discretize the computational domain. This grid was found sufficiently large to ensure that the numerical solution does not depend on the spatial discretization of the computational domain.

The equations are solved using the open-source laminarSMOKE framework,⁵⁰ a CFD code specifically conceived to solve multidimensional laminar reacting flows with detailed kinetic mechanisms. After their discretization through the finite volume technique, the transport equations are solved using the operator-splitting algorithm. The transport (convection and diffusion) step is solved using the backward or implicit Euler's method. The chemical step (corresponding to a set of independent, stiff ODE systems) is solved using the BzzOde solver.⁵¹ Only the species and energy equations are

solved through the operator-splitting algorithm. Since the continuity and the momentum equations are solved in a segregated approach, in order to ensure the conservation of mass at each time step, the PISO algorithm is applied.⁵² Because of the large number of species considered in the kinetic mechanism, parallel solution methods are necessary. The domain decomposition method (DDM) was here adopted. A more detailed description of the laminarSMOKE framework is available in the work of Cuoci et al.⁵³

An Infiniband platform was used for running all the simulations. In its current configuration, it is made up of 16 nodes, each of them having 36 GB of RAM memory and 12 Intel Xeon XS675 (12Mb cache, 3.06 GHz, 6.40 GT/s Intel QPI) processors. The simulations reported in the following were performed using a centered spatial scheme and a maximum Courant number of 0.1.

Figures 16 and 17 report the calculated maps of temperature and mass fractions of selected species for the *n*-heptane and *n*-dodecane flames, respectively. In particular on the left side of

Table 3. Analysis of the CPU Times [Milliseconds per Single Cell] for the Different Parts of the LaminarSMOKE Code

kinetic scheme	species	reactions	Nc7h16 flame			Nc12h26 flame		
			reaction	transport prop.	transport	reaction	transport prop.	transport
Reduced-Nc7h16	100	1567	11.66	0.67	2.75			
Reduced-Nc12h26	120	1930				17.92	0.95	3.92
Polimi_Ht1212	198	6274	76.52	2.62	11.09	77.59	2.51	11.35
Polimi_Tot1212	435	13495	378.41	11.93	57.58	382.96	11.54	59.55
Polimi_Tot1212nox	466	14592	445.78	14.01	79.65	448.1	13.97	78.34

each map, the results corresponding to the reduced kinetic scheme are reported, while on the right side the results obtained using the original kinetic scheme are shown. The typical features of nonpremixed flames can be observed, with fuel inside the flame front and oxidizer (O_2) outside it, together with conversion to CO and H_2 and then to CO_2 and H_2O across the flame front. The reduced mechanism results are in good agreement with the original kinetic scheme, not only in terms of temperature, but also for major species (CO_2 , H_2O , CO). Some discrepancies can be observed for minor species, like CH_2O and CH, especially for the *n*-heptane flame. However, the overall agreement is satisfactory and for both the flames, the reduced model is able to correctly capture the O_2 entrainment at the flame base.

As already reported, the flame lift-off height (here defined as the lowest axial location where the flame reaches the temperature of 1000 K) is a very important property to test the reliability and the accuracy of a kinetic mechanism. In particular, it was demonstrated that the lift-off height is usually strongly dependent on the extinction strain rate of the mechanism.⁴⁹ From the results reported in Figure 16 for the *n*-heptane flame, a good agreement between the calculated flame lift-off heights is evident: in particular, the reduced kinetic scheme predicts a lift-off height of 4.6 mm, while a lift-off height of 5 mm is predicted by the original model. Similarly, for the *n*-dodecane flame the predicted lift-off heights are equal to 2.1 and 2.3 mm for the reduced and the original mechanisms, respectively. The differences are less than 10%, which can be considered a quite satisfactory result and a further demonstration of the reliability of the reduced kinetic mechanisms here proposed.

The final goal of reduction of kinetic mechanisms is to make possible the numerical simulation of complex, multidimensional systems, by reducing the amount of computational resources and computational time. Thus, the analysis of the required CPU time for performing the simulations described above was performed, to better show the benefits behind the reduction of the original kinetic scheme. The laminarSMOKE framework is organized in three main parts: (i) the chemical step, in which uncoupled, stiff ODE systems are integrated over the chosen time-step; (ii) the evaluation of transport properties (mass diffusion coefficients, thermal conductivity, dynamic viscosity, and thermal diffusion coefficients); (iii) the transport (convection and diffusion) step. The CPU times of these three parts are strongly affected by the complexity (number of species) of the kinetic mechanism adopted. Table 3 reports the computational costs for simulating on a single processor a time interval of 10^{-5} s on the mesh described in the previous section. As expected, the CPU time increases for all the parts with the number of species. The reaction step results to be the most consuming part of the code, independently of the kinetics, requiring more than 80–85% of the total computational time. The evaluation of the transport properties and the transport

step cover the 3–5% and the 10% of the total time, respectively. Figure 18 better shows these trends: it can be

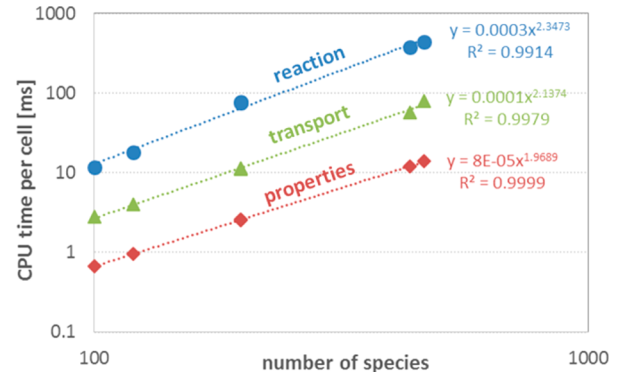


Figure 18. Analysis of the CPU times for the different phases of the laminarSMOKE code for different number of species in the adopted kinetic mechanism. The CPU times reported on the vertical axis refers to a single computational cell.

observed that the CPU time of the reaction steps increases more than quadratically (~ 2.4) with respect to the number of species, while the evaluation of transport properties and the transport step with a power of ~ 2 . This means that by increasing the number of species, the relative weight of the reaction step increases (as evident from Table 3). The overall CPU time increases with a power of ~ 2.3 with respect to the number of species. Thus, since the reduced *n*-heptane mechanism involves only 100 species (less than one-fourth of the species in the original kinetic mechanism), its computational cost is ~ 35 times smaller than the original mechanism. Similarly, for *n*-dodecane the reduction is equal to a factor of ~ 23 . If we suppose that these trends are not affected by the type of kinetic scheme, but only by the number of species, the computational cost of same simulation of the *n*-dodecane flame performed with the LLNL detailed kinetic mechanism (1282 species) would be more than ~ 200 higher than the reduced kinetic mechanism (120 species).

8. CONCLUSIONS

The reduced kinetic mechanisms for *n*-heptane and *n*-dodecane oxidation were assembled and made available from the overall lumped mechanism POLIMI_1212 by simply applying the proposed reduction method without introducing any empirical approximation or kinetic adjustment.

The reduction procedure takes great advantage from the lumping approach proposed for the detailed mechanism. Lumped schemes retain in their formulation the whole degradation pathways of large radicals, saving the important information with a limited number of species and radicals. Aiming to a minimum amount of components, which still allows the reduced mechanism to perform very similar to the

original one in a wide range of conditions, the resulting simplified scheme is then only 3–4 times smaller than the original ones, differently from very detailed kinetic schemes, whose reduced models are up to 10 times smaller, thus sacrificing a larger number of chemical information.

The resulting reduced models of *n*-heptane and *n*-dodecane showed effective in laminar flow systems. Burning velocities is a typical example of problem, which can be solved only with a reasonable number of species. Reduced kinetic schemes make possible the numerical simulation of complex, multidimensional systems, like laminar coflow flames. It was shown that very similar results between detailed and reduced kinetic schemes can be obtained also in the case of the prediction of the lift-off height, very sensitive to the chemistry, with a CPU time reduction of about 35 times, when the reduced model is adopted.

Applications in the field of internal combustion engines, further showed the importance of such reductions, when multizone models are adopted to simulate the combustion chamber.⁵⁴

Further and even more important advantages are expected in the CFD simulations, where the number of species becomes the simulation constraint. In this case, further reduction phases could be obtained by applying a sensitivity analysis on specific targets the reduced model must comply. Such a similar approach has already been implemented, for example, as an extension of DRG method (DRGASA: DRG-aided sensitivity analysis).^{55,56}

What is discussed here for *n*-heptane and *n*-dodecane becomes much more important for heavier complex fuels, like fuel oils or biofuels. In these cases the number of possible isomers prevent any detailed descriptions of the oxidation. Strong lumping procedures have to be adopted before and reduction techniques are also successively necessary. The complexity of these fuels also lies in the difficulty of a proper characterization of the reacting mixtures⁶ often not reproducible, which requires the formulation of surrogate mixtures, whose combustion modeling is a further challenge for lumping and reduction techniques.

■ ASSOCIATED CONTENT

Reduced kinetic schemes of *n*-heptane and *n*-dodecane oxidation. This material is available free of charge via Internet

■ AUTHOR INFORMATION

Corresponding Author

*Phone: +39 02 2399 3250. Fax: +39 02 7063 8173. E-mail: eliseo.ranzi@polimi.it.

Notes

The authors declare no competing financial interest.

■ ACKNOWLEDGMENTS

This work was carried out through the financial support of the European Union (EU) as part of the EMICOPTER Project (CS-GA-2009-1261 251798).

■ REFERENCES

(1) Lu, T. F.; Law, C. K. Toward accommodating realistic fuel chemistry in large-scale computations. *Prog. Energy Combust. Sci.* **2009**, *35* (2), 192–215.

(2) Smith, G. P.; Golden, D. M.; Frenklach, M.; Moriarty, N. W.; Eiteneer, B.; Goldenberg, M.; Bowman, C. T.; Hanson, R. K.; Song, S.; Gardiner, W. C.; Lissianski, V. V.; Qin, Z. *GRI 3.0 Kinetic Mechanism*. http://www.me.berkeley.edu/gri_mech/.

(3) Chemical-Kinetic Mechanisms for Combustion Applications. <http://web.eng.ucsd.edu/mae/groups/combustion/mechanism.html> (accessed Oct. 2013).

(4) Westbrook, C. K.; Pitz, W. J.; Herbinet, O.; Curran, H. J.; Silke, E. J. A comprehensive detailed chemical kinetic reaction mechanism for combustion of n-alkane hydrocarbons from n-octane to n-hexadecane. *Combust. Flame* **2009**, *156* (1), 181–199.

(5) Herbinet, O.; Pitz, W. J.; Westbrook, C. K. Detailed chemical kinetic oxidation mechanism for a biodiesel surrogate. *Combust. Flame* **2008**, *154* (3), 507–528.

(6) Huang, H.; Fairweather, M.; Griffiths, J. F.; Tomlin, A. S.; Brad, R. B. A systematic lumping approach for the reduction of comprehensive kinetic models. *Proc. Combust. Inst.* **2005**, *30*, 1309–1316.

(7) Altgelt, K. H.; Boduszynski, M. M. *Composition and analysis of heavy petroleum fractions*; M. Dekker: New York, 1994; Part ix, p 495.

(8) Oehlschlaeger, M. A.; Shen, H. P. S.; Frassoldati, A.; Pierucci, S.; Ranzi, E. Experimental and kinetic modeling study of the pyrolysis and oxidation of decalin. *Energy Fuels* **2009**, *23* (3), 1464–1472.

(9) Fournet, R.; Warth, V.; Glaude, P. A.; Battin-Leclerc, F.; Scacchi, G.; Côme, G. M. Automatic reduction of detailed mechanisms of combustion of alkanes by chemical lumping. *Int. J. Chem. Kinetics* **2000**, *32* (1), 36–51.

(10) Ranzi, E.; Dente, M.; Goldaniga, A.; Bozzano, G.; Faravelli, T. Lumping procedures in detailed kinetic modeling of gasification, pyrolysis, partial oxidation and combustion of hydrocarbon mixtures. *Prog. Energy Combust. Sci.* **2001**, *27* (1), 99–139.

(11) Westbrook, C. K.; Warnatz, J. r.; Pitz, W. J. A detailed chemical kinetic reaction mechanism for the oxidation of iso-octane and n-heptane over an extended temperature range and its application to analysis of engine knock. *Symp. (Int.) Combust.* **1989**, *22* (1), 893–901.

(12) Chevalier, C.; Pitz, W. J.; Warnatz, J.; Westbrook, C. K.; Melenk, H. Hydrocarbon ignition: Automatic generation of reaction mechanisms and applications to modeling of engine knock. *Symp. (Int.) Combust.* **1992**, *24* (1), 93–101.

(13) Steele Jr., G. L.; Richard, P. G. The evolution of Lisp. In *The second ACM SIGPLAN conference on History of programming languages*; ACM: New York, NY, 1993; pp 231–270.

(14) Blurock, E. S. Reaction: System for Modeling Chemical Reactions. *J. Chem. Inf. Comput. Sci.* **1995**, *35* (3), 607–616.

(15) Ranzi, E.; Faravelli, T.; Gaffuri, P.; Sogaro, A. Low-Temperature Combustion - Automatic-Generation of Primary Oxidation Reactions and Lumping Procedures. *Combust. Flame* **1995**, *102* (1–2), 179–192.

(16) Come, G. M.; Warth, V.; Glaude, P. A.; Fournet, R.; Battin-Leclerc, F.; Scacchi, G. Computer-aided design of gas-phase oxidation mechanisms - Application to the modeling of n-heptane and iso-octane oxidation. *Symp. (Int.) Combust.* **1996**, *26* (1–2), 755–762.

(17) Broadbelt, L. J.; Stark, S. M.; Klein, M. T. Computer generated reaction modelling: Decomposition and encoding algorithms for determining species uniqueness. *Comput. Chem. Eng.* **1996**, *20* (2), 113–129.

(18) Susnow, R. G.; Dean, A. M.; Green, W. H.; Peczak, P.; Broadbelt, L. J. Rate-based construction of kinetic models for complex systems. *J. Phys. Chem. A* **1997**, *101* (20), 3731–3740.

(19) Warth, V.; Battin-Leclerc, F.; Fournet, R.; Glaude, P. A.; Come, G. M.; Scacchi, G. Computer based generation of reaction mechanisms for gas-phase oxidation. *Comput. Chem.* **2000**, *24* (5), 541–560.

(20) Matheu, D. M.; Dean, A. M.; Grenda, J. M.; Green, W. H.

Mechanism generation with integrated pressure dependence: A new model for methane pyrolysis. *J. Phys. Chem. A* **2003**, *107* (41), 8552–8565.

(21) Glaude, P. A.; Battin-Leclerc, F.; Fournet, R.; Warth, V.; Come, H. M.; Scacchi, G. Construction and simplification of a model for the oxidation of alkanes. *Combust. Flame* **2000**, *122* (4), 451–462.

- (22) Dagaut, P.; Reuillon, M.; Cathonnet, M. High Pressure Oxidation of Liquid Fuels From Low to High Temperature. 1. n-Heptane and iso-Octane. *Combust. Sci. Technol.* **1993**, *95* (1–6), 233–260.
- (23) Lindstedt, R. P.; Maurice, L. Q. Detailed kinetic modelling of n-heptane combustion. *Combust. Sci. Technol.* **1995**, *107* (4–6), 317–353.
- (24) Curran, H. J.; Gaffuri, P.; Pitz, W. J.; Westbrook, C. K. A Comprehensive Modeling Study of n-Heptane Oxidation. *Combust. Flame* **1998**, *114* (1,Ä2), 149–177.
- (25) Simmie, J. M. Detailed chemical kinetic models for the combustion of hydrocarbon fuels. *Prog. Energy Combust. Sci.* **2003**, *29* (6), 599–634.
- (26) Battin-Leclerc, F. Detailed chemical kinetic models for the low-temperature combustion of hydrocarbons with application to gasoline and diesel fuel surrogates. *Prog. Energy Combust. Sci.* **2008**, *34* (4), 440–498.
- (27) Zádor, J.; Taatjes, C. A.; Fernandes, R. X. Kinetics of elementary reactions in low-temperature autoignition chemistry. *Prog. Energy Combust. Sci.* **2011**, *37* (4), 371–421.
- (28) Kouri, T. M.; Crabtree, J. D.; Huynh, L.; Dean, A. M.; Mehta, D. P. RCARM: Reaction classification using automated reaction mapping. *Int. J. Chem. Kinetics* **2013**, *45* (2), 125–139.
- (29) Ranzi, E.; Frassoldati, A.; Granata, S.; Faravelli, T. Wide-range kinetic modeling study of the pyrolysis, partial oxidation, and combustion of heavy n-alkanes. *Ind. Eng. Chem. Res.* **2005**, *44* (14), 5170–5183.
- (30) Jacob, S. M.; Gross, B.; Voltz, S. E.; Weekman, V. W. A lumping and reaction scheme for catalytic cracking. *AIChE J.* **1976**, *22* (4), 701–713.
- (31) Turanyi, T.; Berces, T.; Vajda, S. Reaction-Rate Analysis of Complex Kinetic Systems. *Int. J. Chem. Kinetics* **1989**, *21* (2), 83–99.
- (32) Li, G.; Rabitz, H. A General-Analysis of Exact Lumping in Chemical-Kinetics. *Chem. Eng. Sci.* **1989**, *44* (6), 1413–1430.
- (33) Tomlin, A. S.; Turányi, T.; Pilling, M. J., Mathematical tools for the construction, investigation and reduction of combustion mechanisms. In *Comprehensive Chemical Kinetics*; Pilling, M. J., Ed. Elsevier, 1997; Vol. 35, pp 293–437.
- (34) Wei, J.; Kuo, J. C. W. Lumping Analysis in Monomolecular Reaction Systems. Analysis of the Exactly Lumpable System. *Ind. Eng. Chem. Fundam.* **1969**, *8* (1), 114–123.
- (35) Ranzi, E.; Frassoldati, A.; Grana, R.; Cuoci, A.; Faravelli, T.; Kelley, A. P.; Law, C. K. Hierarchical and comparative kinetic modeling of laminar flame speeds of hydrocarbon and oxygenated fuels. *Prog. Energy Combust. Sci.* **2012**, *38* (4), 468–501.
- (36) Ciezki, H. K.; Adomeit, G. Shock-tube investigation of self-ignition of n-heptane-air mixtures under engine relevant conditions. *Combust. Flame* **1993**, *93* (4), 421–433.
- (37) Vasu, S. S.; Davidson, D. F.; Hong, Z.; Vausdevan, V.; Hanson, R. K. n-Dodecane oxidation at high-pressures: Measurements of ignition delay times and OH concentration time-histories. *Proc. Combust. Inst.* **2009**, *21* (1), 173–180.
- (38) Davidson, D. F.; Hong, Z.; Pilla, G. L.; Farooq, A.; Cook, R. D.; Hanson, R. K. Multi-species time-history measurements during n-dodecane oxidation behind reflected shock waves. *Proc. Combust. Inst.* **2011**, *33* (1), 151–157.
- (39) Ranzi, E.; Gaffuri, P.; Faravelli, T.; Dagaut, P. A Wide-Range Modeling Study of n-Heptane Oxidation. *Combust. Flame* **1995**, *103* (1–2), 91–106.
- (40) Mze-Ahmed, A.; Hadj-Ali, K.; Dagaut, P.; Dayma, G. Experimental and Modeling Study of the Oxidation Kinetics of n-Undecane and n-Dodecane in a Jet-Stirred Reactor. *Energy Fuels* **2012**, *26* (7), 4253–4268.
- (41) Li, B.; Liu, N.; Zhao, R.; Egolfopoulos, F. N.; Zhang, H. Extinction Studies of Flames of Heavy Neat Hydrocarbons and Practical Fuels. *J. Propul. Power* **2013**, *29* (2), 352–361.
- (42) Wang, H.; Dames, E.; Sirjean, B.; Sheen, D. A.; Tangko, R.; Violi, A.; Lai, J. Y. W.; Egolfopoulos, F. N.; Davidson, D. F.; Hanson, R. K.; Bowman, C. T.; Law, C. K.; Tsang, W.; Cernansky, N. P.; Miller, D. L.; Lindstedt, R. P. JetSurF version 2.0: A high-temperature chemical kinetic model of n-alkane (up to n-dodecane), cyclohexane, and methyl-, ethyl-, n-propyl and n-butyl-cyclohexane oxidation at high temperatures. <http://melchior.usc.edu/JetSurF/JetSurF2.0>, 2010 (accessed Oct. 2013).
- (43) Li, B.; Zhang, H.; Egolfopoulos, F. N. Laminar flame propagation of atmospheric iso-cetane/air and decalin/air mixtures. *Combust. Flame* **2014**, *161* (1), 154–161.
- (44) Wang, H.; Frenklach, M. Detailed Reduction of Reaction-Mechanisms for Flame Modeling. *Combust. Flame* **1991**, *87* (3–4), 365–370.
- (45) Lu, T. F.; Law, C. K. Linear-time reduction of large kinetic mechanisms with directed relation graph: n-heptane and iso-octane. *Combust. Flame* **2005**, *144*, 24–36.
- (46) D’Errico, G.; Lucchini, T.; Stagni, A.; Frassoldati, A.; Faravelli, T.; Ranzi, E. *Reduced Kinetic Mechanisms for Diesel Spray Combustion Simulations*. SAE Technical Paper, 2013.
- (47) Saggese, C.; Frassoldati, A.; Cuoci, A.; Faravelli, T.; Ranzi, E. A lumped approach to the kinetic modeling of pyrolysis and combustion of biodiesel fuels. *Proc. Combust. Inst.* **2013**, *34* (1), 427–434.
- (48) Tosatto, L.; Bennett, B. A. V.; Smooke, M. D. Comparison of different DRG-based methods for the skeletal reduction of JP-8 surrogate mechanisms. *Combust. Flame* **2013**, *160*, 1572–1582.
- (49) Mohammed, R. H.; Tanoff, M. A.; Smooke, M. D.; Shaffer, A. M. Computational and experimental study of a forced, time-varying, axisymmetric, laminar diffusion flame. *Proc. Combust. Inst.* **1998**, *27*, 693–702.
- (50) Cuoci, A.; Frassoldati, A.; Faravelli, T.; Ranzi, E. A computational tool for the detailed kinetic modeling of laminar flames: Application to C₂H₄/CH₄ coflow flames. *Combust. Flame* **2013**, *160* (5), 870–886.
- (51) Buzzi-Ferraris, G.; Manca, D. BzzOde: a new C++ class for the solution of stiff and non-stiff ordinary differential equation systems. *Comput. Chem. Eng.* **1998**, *22* (11), 1595–1621.
- (52) Issa, R. I. Solution of the Implicitly Discretized Fluid Flow Equation by Operator Splitting. *J. Comput. Phys.* **1986**, *62*, 40–65.
- (53) Cuoci, A.; Frassoldati, A.; Faravelli, T.; Ranzi, E. Numerical modeling of laminar flames with detailed kinetics based on the operator-splitting method. *Energy Fuels* **2013**, DOI: 10.1021/ef4016334.
- (54) Bissoli, M.; Cuoci, A.; Frassoldati, A.; Faravelli, C.; Ranzi, E.; Lucchini, T.; D’Errico, G.; Contino, F. Detailed Kinetic Analysis of HCCI Combustion Using a New Multi-Zone Model and CFD Simulations. *SAE Int. J. Engines* **2013**, *6* (3), 1594–1609.
- (55) Zheng, X. L.; Lu, T. F.; Law, C. K. Experimental counterflow ignition temperatures and reaction mechanisms of 1,3-butadiene. *Proc. Combust. Inst.* **2007**, *31* (1), 367–375.
- (56) Lu, T.; Law, C. K. Strategies for mechanism reduction for large hydrocarbons: n-heptane. *Combust. Flame* **2008**, *154* (1), 153–163.
- (57) Dagaut, P.; Reuillon, M.; Cathonnet, M. Experimental study of the oxidation of n-heptane in a jet stirred reactor from low to high temperature and pressures up to 40 atm. *Combust. Flame* **1995**, *101* (1), 132–140.
- (58) Kumar, K.; Sung, C. J. Laminar flame speeds and extinction limits of preheated n-decane/O₂/N₂ and n-dodecane/O₂/N₂ mixtures. *Combust. Flame* **2007**, *151* (1–2), 209–224.
- (59) Davis, S. G.; Law, C. K. Determination of and Fuel Structure Effects on Laminar Flame Speeds of C₁ to C₈ Hydrocarbons. *Combust. Sci. Technol.* **1998**, *140* (1–6), 427–449.
- (60) Ji, C. S.; Dames, E.; Wang, Y. L.; Wang, H.; Egolfopoulos, F. N. Propagation and extinction of premixed C-5-C-12 n-alkane flames. *Combust. Flame* **2010**, *157* (2), 277–287.